Wave propagation in granular assemblies

Stephan Melin*
Höchstleistungsrechenzentrum, Forschungszentrum KFA–Jülich G.m.b.H., Postfach 1913, D-52425 Jülich, Germany
(Received 27 May 1993)

In order to achieve a better understanding of the properties of granular media in a dense packing, the propagation of sound in such systems is studied numerically. In this paper, I study the depth dependence of the sound propagation speed in granular media for a single pulse. I find that for the simulated cases the speed of sound does not behave like the postulated power law. Also, I will discuss the amplitude and phase distribution in a rectangular box if the system is continuously excited. I find a strong localization of the peaks of the amplitudes in accordance with the results for a very simplified model by Leibig [Phys. Rev. E **49**, 1647 (1994)].

PACS number(s): 03.40.Kf, 43.25.+y, 43.40.+s, 83.70.Fn

I. INTRODUCTION

Recent experimental and numerical work shows that sound propagation in sand exhibits very complex behavior. Liu and Nagel [1] reported fluctuations in the acceleration amplitudes measured at several points in the system. The spectrum of the time evolution of these amplitudes revealed a power law. They also measured the frequency response for their systems. The frequency response seems to be a characteristic of the system; a slight rearrangement of the beads revealed a completely different behavior. Leibig [2] calculated the frequency response for a system consisting of spherical balls interacting via linear springs on a quadratic lattice. These numerical results are in agreement with [1].

There have been further predictions about the depth dependence of the sound propagation speed: extrapolating from the power-law dependence of the wave propagation speed from pressure, which has been observed various times (cf. [3] for a more exhaustive reference) for comparatively high pressures, there have been predictions of a so-called "mirage effect" [1,4] for horizontal sound propagation. This means that, on the surface, sound cannot propagate horizontally, thus leading to the effect that an initially vertical wave front bends upwards until it becomes horizontal. In the first part of this paper, I show that these predictions derived from the continuum limit for infinitesimal small amplitudes do not hold for the simulated cases.

In the second part, I apply a continuous excitation to the system. The evolving patterns for the distribution of the amplitudes and phases are very complicated, and seem to confirm the numerical results of Leibig [2]. The spatial distribution of the phases of the vibration in the x direction and the velocity field taken at an arbitrary time conform the result of the first part, that there is indeed no power-law behavior for the depth dependence of the sound velocity.

*Electronic address: melin@hlrserv.hlrz.kfa-juelich.de

II. MODEL AND METHODS USED

The system studied is a two-dimensional packing of grains under gravity. The grains are packed into a rectangular box. To introduce excitations the left wall of this container is vibrated.

For the sake of simplicity I chose the particles to be perfectly spherical. Also, the rotation of the particles is not taken into account. The elastic repulsion between two spheres is given by the Hertz contact law:

$$\mathbf{f}_{ij}^{\text{elastic}} = g[\tfrac{1}{2}(D_i + D_j) - |\mathbf{r}_{ij}|]^{3/2} \frac{\mathbf{r}_{ij}}{|\mathbf{r}_{ij}|} , \tag{1}$$

where $D_i = 2R_i$ is the diameter of the ith particle, and $g = Y/\sqrt{(1/R_i)+(1/R_j)}$ is a prefactor which depends on the elastic constants (here I assume that the elastic properties of all particles are the same, therefore I replaced the expression which depends on the Poisson number E and the elasticity ratio σ by the single constant Y) and the diameters of the spheres [5].

To simulate the inelasticity of the collision I introduce a normal dissipation. I also introduce a shear friction [6]. The energy put in has to be dissipated, because otherwise the system would heat up and "explode." For the dissipation I use the simplest case, where the friction linearly depends on the velocity:

$$\mathbf{f}_{ij}^{\text{diss normal}} = -\gamma_n m_{\text{eff}} (\mathbf{r}_{ij} \cdot \mathbf{v}_{ij}) \frac{\mathbf{r}_{ij}}{|\mathbf{r}_{ij}|} , \tag{2}$$

$$\mathbf{f}_{ij}^{\text{diss tangential}} = -\gamma_s m_{\text{eff}} (\mathbf{t}_{ij} \cdot \mathbf{v}_{ij}) \frac{\mathbf{t}_{ij}}{|\mathbf{t}_{ij}|} , \tag{3}$$

where

$$\mathbf{t}_{ij} = \begin{bmatrix} -r_{ij}^{y} \\ r_{ij}^{x} \end{bmatrix} ,$$

where γ represents the dissipation coefficients and m_{eff} is the effective mass of the two-particle system. These interparticle forces only act when the two particles touch each other:

$\frac{1}{2}(D_i + D_j) \geq |\mathbf{r}_{ij}|$.

If they do not touch, the interparticle forces are zero. All particles are subject to gravity.

To simulate this system I chose a molecular-dynamics technique. The equations of motion for each particle are integrated by using a fifth-order Gear predictor corrector [7]. One of the problems of molecular-dynamics simulations is to determine the particles which interact with each other. A naive approach would be to test whether two particles interact for all possible pairs of particles; this approach scales with N^2, where N is the number of particles. For large systems this approach becomes very ineffective. Since the interactions are short range, it is sufficient to test for possible interactions only with neighboring particles. The determination of the neighborhood of the particle and the optimized implementation on various architectures has been extensively covered in the literature (cf. [7–10]).

However, if one places equally sized spheres into a rectangular box, they can arrange in a dense sphere packing. In the two-dimensional case the centers of these spheres will be on a triangular lattice. If one now applies a small perturbation (e.g., a weak polydispersity or a small vibration) the topology of this packing will not be destroyed. On the triangular lattice each particle has six neighbors, since the neighbors are fixed throughout the whole simulation the time-consuming part of determining of the possible interaction partners can be avoided. This triangular lattice can be mapped very easily onto a square lattice, thus allowing us to put each particle on a single virtual processor on a CM2 computer.

In order to simulate the interaction with the walls of the box, I confined the possible motion of the boundary particles. The bottom particles are allowed to move in the x direction only, and the particles forming the sidewalls can move only in the y direction.

III. DEPTH DEPENDENCE OF THE WAVE PROPAGATION SPEED

There are calculations [3] which state that the wave propagation velocity v_c is dependent on the pressure p like $v_c \propto p^{1/6}$ if the elastic interaction is the Hertz contact law. For high pressures the pressure dependence of the sound propagation speed has been verified experimentally (cited in [3]). For low pressures, however, another contact law has been found experimentally, so that $v_c \propto p^{1/4}$; this is not only true for sands, but can also be true for sphere packings at certain parameters (see [3] and the references therein for a more detailed discussion).

If one now packs the spheres inside a box and does not apply any external forces on the packing except for gravity, it can be argued that the average pressure increases linearly with the depth h, thus leading to the relationship $v_c \propto h^{1/6}$. This, however, means that the wave velocity approaches zero near the surface, so that a plane wave which travels horizontally at some time $t=0$ will start to bend up, creating a so-called "mirage effect," as predicted in [1,4]. As Liu and Nagel observed, "such an analysis might be much too simple, since real sand is not homogeneous but granular." Surprisingly enough, I have not found any reference to experiments observing this mirage effect.

Looking at the contact network reveals that arguments leading to the prediction of a "mirage effect" do not take into account the directional anisotropy of the contact forces. The strength of the contacts between particles increases with depth, but not necessarily in an isotropic fashion. In a regular arrangement of monodisperse spheres, the strength of the vertical contacts (to be exact, the ones which point downwards in a 60° angle) increases linearly with depth, but the horizontal contacts remain negligible. This means that the particles barely touch but the elastic force between them is zero, as one can see in

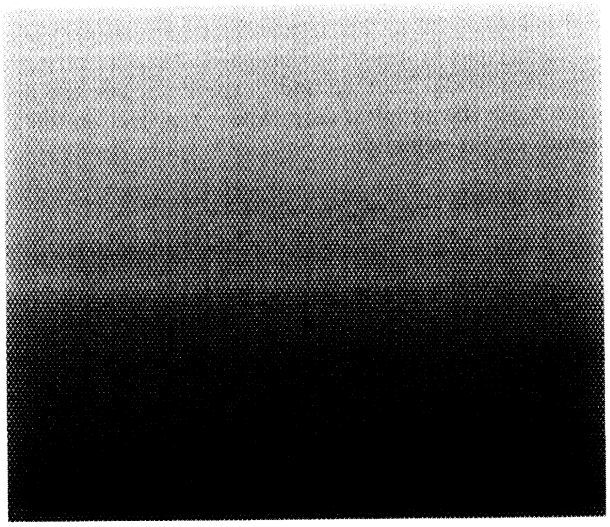

monodisperse

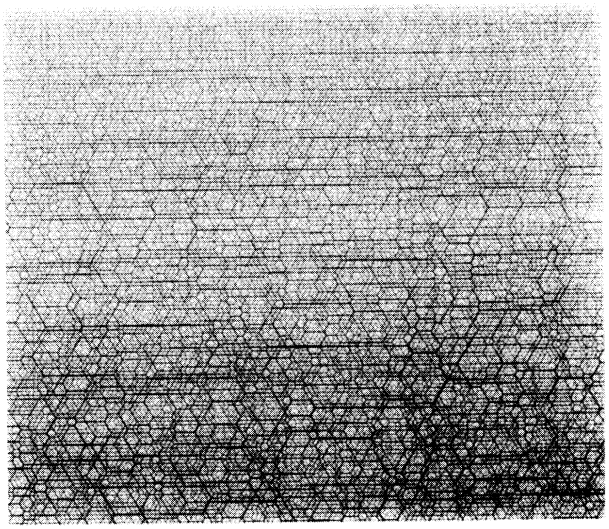

polydisperse

FIG. 1. These are excerpts from the contact network for an equilibrated 256×256 packing of spheres; the thickness codes the strength of the bonds. For the monodisperse case one can see that there are no horizontal bonds. Although the particles touch each other, there are no elastic forces between them. For the polydisperse case it is completely different; there are horizontal bonds.

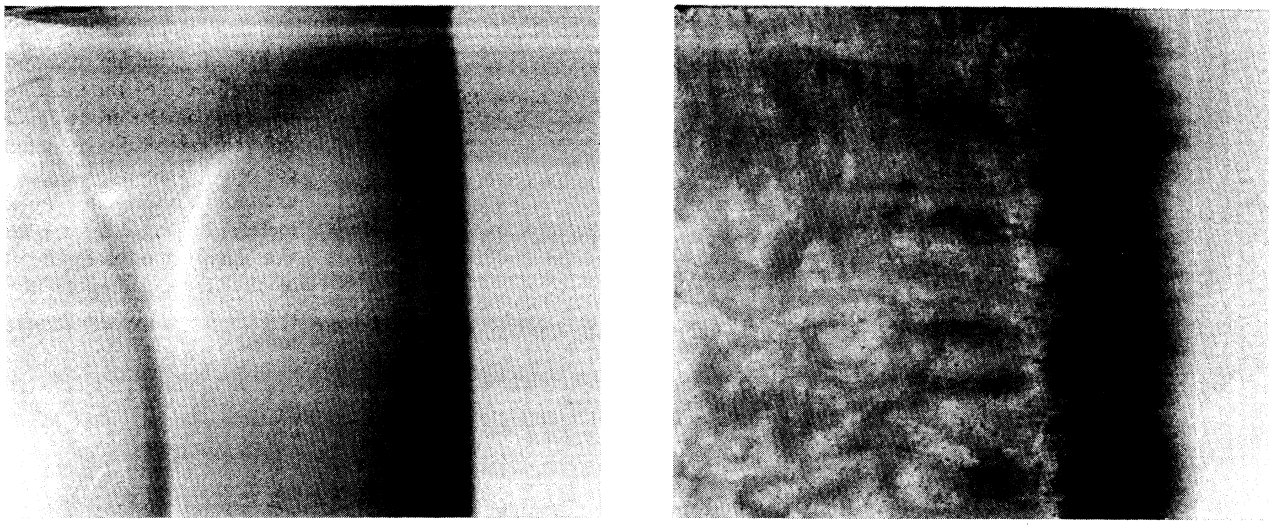

FIG. 2. Here one can see the position of the wave front shortly before the wave hits the opposite wall in the system. The gray scales code the kinetic energy of the particles (dark means high kinetic energy). The amplitude is $0.01D$. The left figure shows the monodisperse case, and the right figure shows the polydisperse case. The main qualitative difference between these two figures is that in the polydisperse case the front is not smooth as in the monodisperse case. The structures behind the wave front are due to internal reflection of the wave. The secondary wave front in the monodisperse case is created at the beginning of the simulation and travels (due to its lower amplitude) much more slowly than the primary wave front.

Fig. 1 (this is only strictly true if one disregards the horizontal deformation of the spheres under vertical pressure). Any finite vertical excitation of the particles will, however, close the contacts between horizontally neighboring particles, thus allowing horizontal sound propagation. Therefore it seems very unlikely that the depth dependence of the sound propagation speed really follows the simple law $v_c \propto h^{1/6}$. Moreover the propagation speed of a single pulse will be dependant on its amplitude. Since there is dissipation the amplitude changes with time, so the propagation speed will also be time dependent.

To measure the dependence of the wave speed on the depth, I simulated a two-dimensional system consisting of 256×256 monodisperse spheres under gravity. On one side, I applied a step-shaped excitation; this means that all spheres at this wall are instantaneously moved a small distance to the side. In the left part of Fig. 2 one can see that there is indeed a dependence of the wave propagation speed on the depth; however, this dependence is very weak. One can easily see that the relation $v_c \propto h^{1/6}$ cannot be true for this case, because the wave near the surface has traveled a considerable distance. To quantify this behavior I measured the position of the wave front for every time step. As the position of the wave front I chose particles which have maximum total energy (kinetic and elastic) on a given layer (equal to height). As one can clearly see in Fig. 3, the anticipated depth depen-

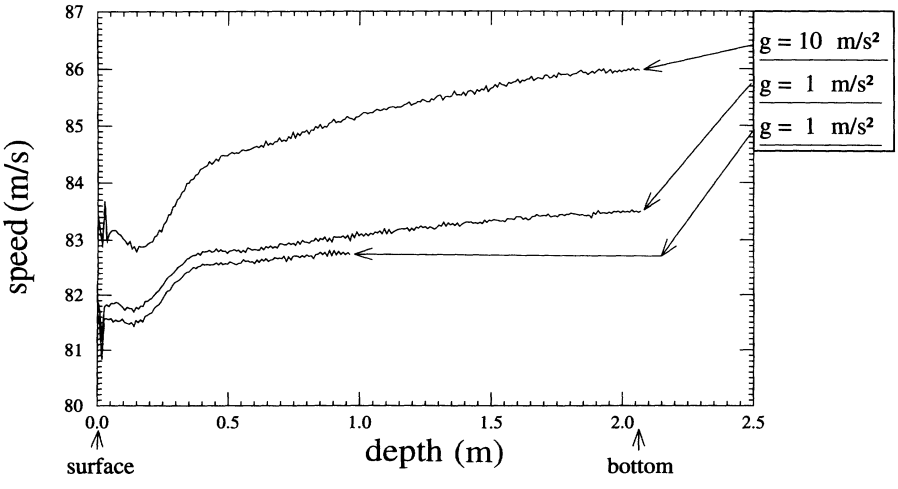

FIG. 3. This figure shows the depth dependence of the wave velocity for two different gravities approximately 7.8 ms after the pulse. The third curve for a system of 256×128 particles (i.e., half the height) shows that the way I have implemented the bottom boundary has very little effect on the shape of the curves (to illustrate this, I have subtracted 0.25 m/s from this curve).

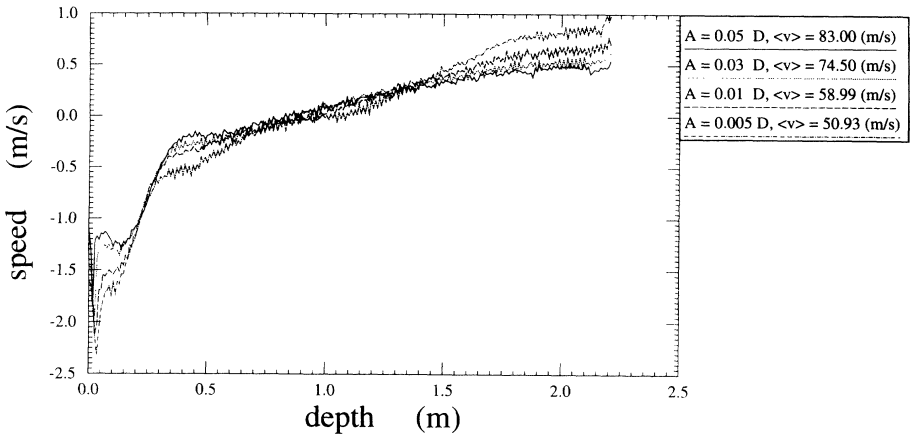

FIG. 4. This figure shows the normalized (i.e., the mean velocity $\langle v \rangle$ of the front for each different amplitude is subtracted) wave velocity for different excitation amplitudes approximately 7.8 ms after the pulse. For small amplitudes the slope of the curve starts to diverge from the slope for higher amplitudes.

dence of $v_c \propto h^{1/6}$ does not hold true for the simulated cases. The depth dependence increases for higher gravitation. Moreover, the propagation velocity of the wave front depends very much upon the amplitude of the initial excitation. Closer examination of the velocities for the same system with different amplitudes reveals that the curves are parallel for reasonably high amplitudes, as one can seen in Fig. 4. The explanation for this behavior is that there are two competing propagation paths: The first is the propagation of the wave along the 60° bonds which exist in the equilibrated system (see Fig. 1); the strengths of these couplings vary with height. The second path is along the horizontal bonds which have zero strength in the equilibrated system, but will be closed as soon as the system is excited. The strength of this coupling is independent of the height. For small amplitudes, however, this second mechanism becomes less important, and the first one will dominate. One can see this in Fig. 4 for the curve for $A = 0.005D$ (in this case, A means amplitude and D means diameter of the particles) whose slope starts to deviate from the slopes of the other curves.

The second mechanism also leads to an explanation of why sound can propagate horizontally even on the surface. The particles touch each other but do not exert any force on each other (I neglect the very weak horizontal forces due to the deformation caused by gravitation and the pressure from the particles above, making this argument also valid for systems where the particles touch but do not exert any force on each other, i.e., when the pressure is zero). If one now applies a *finite* perturbation on the system, bonds will start to appear, thus allowing propagation of sound in any direction. Thus the power laws for the pressure dependence of the wave propagation speed will break down for low pressures. The propagation speed will be determined by the amplitude of the wave, and the gap which has to be closed between adjacent particles so that they can interact.

Looking at the time evolution of the wave propagation speed in Fig. 5 reveals that the wave speed decreases with time. The explanation for this can be found in Figs. 2 and 4. In (the left part of) Fig. 2 one can see that although the wave front is very sharp, the particles in the region behind the wave front still have a great deal of kinetic energy remaining. This means that the total energy in the wave front decreases with time, since some of the energy of the wave front is lost (for the wave front) in the region which has been traversed. A second effect is that due to the dissipative terms some of the kinetic energy is lost. In Fig. 4 one can see that for smaller initial energies the wave speed is also smaller.

One could argue that these arguments are only valid for the monodisperse case, and that for a polydisperse case there will be a significant deviation from observa-

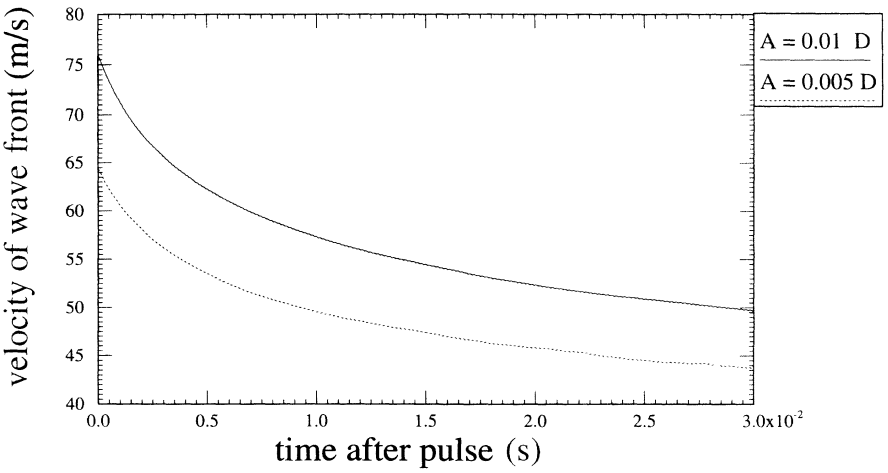

FIG. 5. The two curves show the time evolution for the velocity of the wave front at a single depth for two different amplitudes.

tions made for the monodisperse case. However, a visual comparison between the wave propagation in the monodisperse and polydisperse cases (here I have used a polydispersity of $\Delta A_{\max} = \pm 0.01 A$, where $A = R^2$) shows no qualitative difference in the general behavior (see Fig. 2). The only exception is that there is no longer a well-defined wave front. The reason for this can be seen in the right part of Fig. 1. Due to the polydispersity some of the horizontal bonds are already closed in the equilibrated state. Any excitation will travel faster along these closed bonds; the stronger the bonds, the faster it will travel (the elastic force is *nonlinear).* Since the spatial distribution of the horizontal bonds is different for each layer, there are some parts of the system where the wave front propagates fast on one layer and slow on another, and vice versa in a different region. Globally, however, the two different systems behave very similarly. The reason for this similar behavior is that although the mean value of the overlap between vertically (approximately in a 60° angle) neighboring particles does depend on the depth, the mean overlap between horizontally neighboring particles is not depth dependent (or at least the depth dependence can be neglected).

IV. SOUND PROPAGATION FOR CONTINUOUS EXCITATION

Instead of looking at a single excitation, one could look at the behavior of the system when continuously excited. In experimental work [1,11] it is possible to measure the acceleration amplitudes and phases of a few (detector) particles. The behavior of these measured systems turns out to be extremely complicated. In order to find out whether this behavior is due to the experimental setup or a general property of particulate systems, I again simulated the simplest case.

I performed simulations for the same system which was used for simulations in Sec. III. The system has been driven sinusoidally at a frequency of 100 Hz, and the acceleration amplitude was 0.5 g. The sound source is the particles forming the left wall. Both figures have been taken 256 cycles (2.56 s) after the beginning of the excitation. In Fig. 6 one can see the acceleration amplitudes of the different particles in the monodisperse case. Figure 7 shows the corresponding phases.

The resulting patterns are far from regular. Note the very sharp phase shift on the right side of the system; it extends in a 60° angle downwards. These sharp phase shifts also appeared for different parameters (different geometries, acceleration amplitudes, gravities), but in most cases they disappeared after a while to be replaced by a "noisy" region. The reason for these sharp phase shifts can be seen in Fig. 8. When the oscillation is applied to the system, it starts to expand in the Y direction, but in the area opposite to the wall which excites the system this expansion does not take place; on the contrary, in this area the system shrinks. This creates a fault line where neighboring particles have a small vertical offset. These fault lines extend typically in a 60° angle downwards. Since this is an effect which only occurs for specific parameter values in a monodisperse system, I will not discuss it further.

Comparing the velocity field (see Fig. 8) with the phase field (x direction) (see Fig. 7) reveals that these two are correlated as one would expect; both show the same vertical structure. The structure of these fields does not change very much after some time so that one could speak of a standing wave.

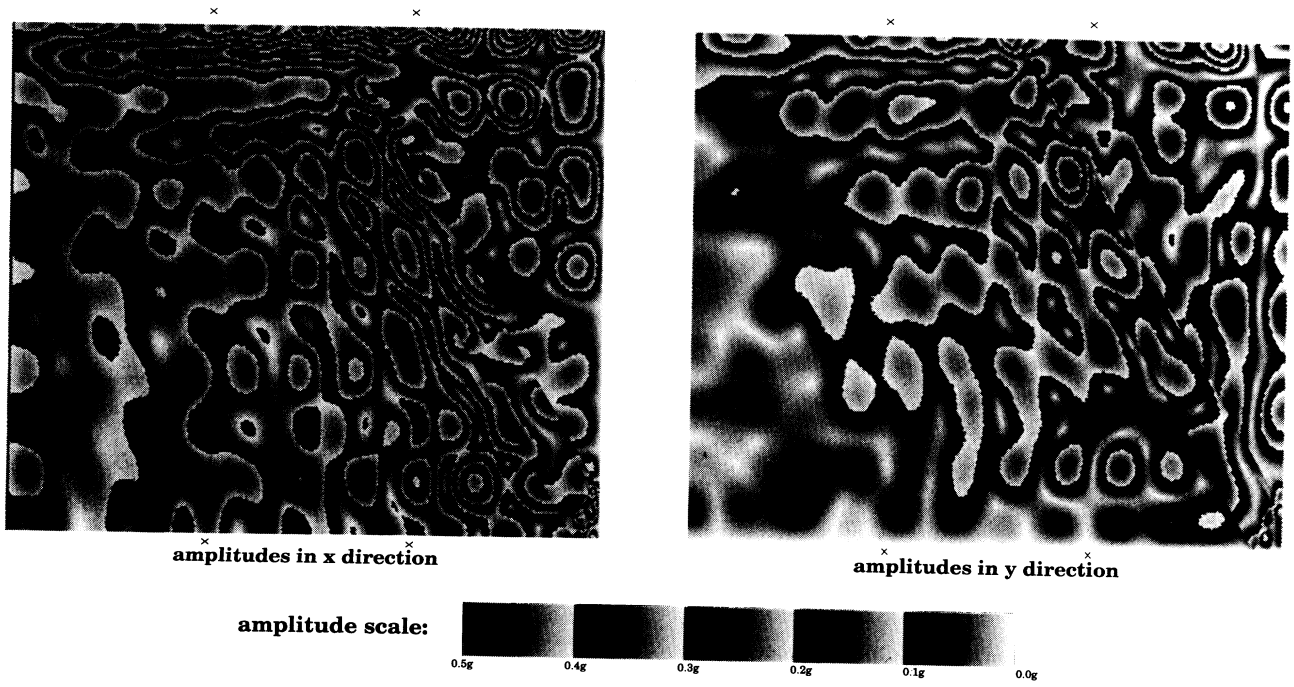

FIG. 6. The contour maps for the acceleration amplitudes of the monodisperse system 2.56 s after the start of the excitation. The left picture shows the acceleration amplitudes of the vibration in the x direction, and the right the amplitudes in the y direction.

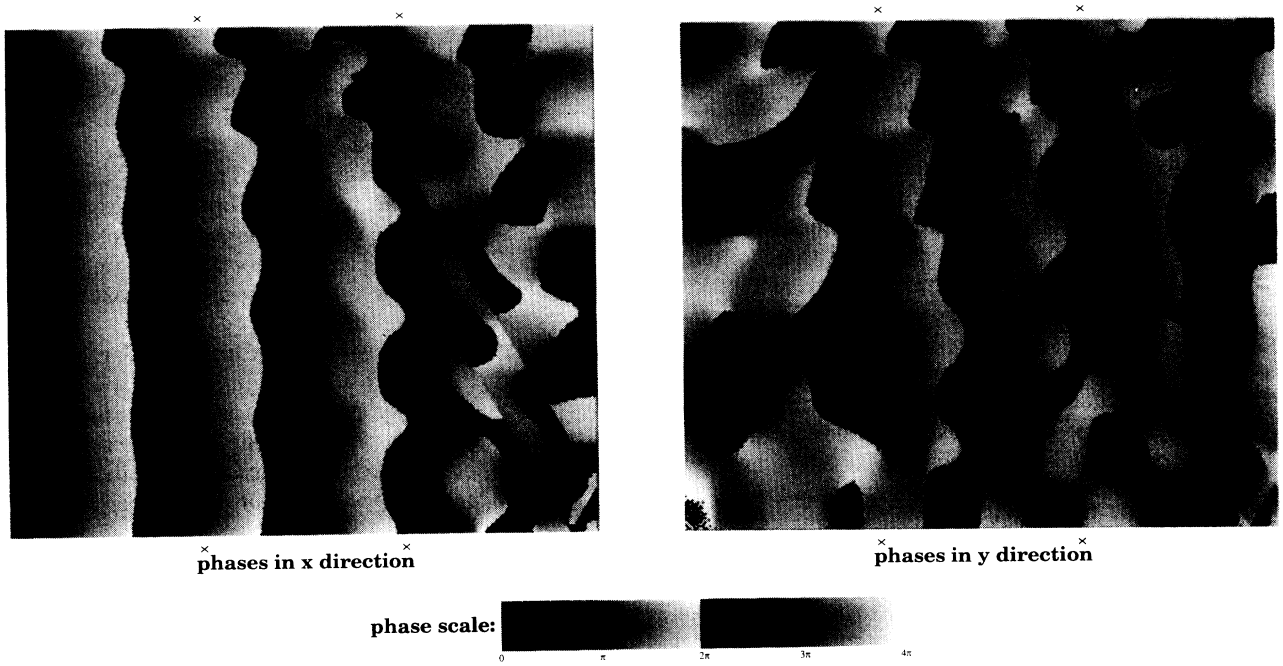

FIG. 7. The acceleration phases for the monodisperse system 2.56 s after the start of the excitation. The left picture shows the phases of the vibration in the x direction, the right one shows the phases of the vibration in y direction.

As I showed in Sec. III, there is very little depth dependence of the sound propagation speed for a single pulse. One can clearly see that also in this case the depth dependence of the wave propagation speed does not behave like the postulated power law. Still there is sound propagation on the surface, and the spatial distribution of the phase (as well as the velocity field) exhibits only vertical structures. In the case of the existence of the "mirage effect" I would expect that regions with coherent phases would bend upwards.

The distribution of the amplitudes reveals an even more complicated structure. The general trend is a decline in the amplitudes (see Fig. 9), but there is a strong localization of the peaks of the amplitudes. The distribution and size of these peaks still changes with time, so that one can assume that this changing will continue

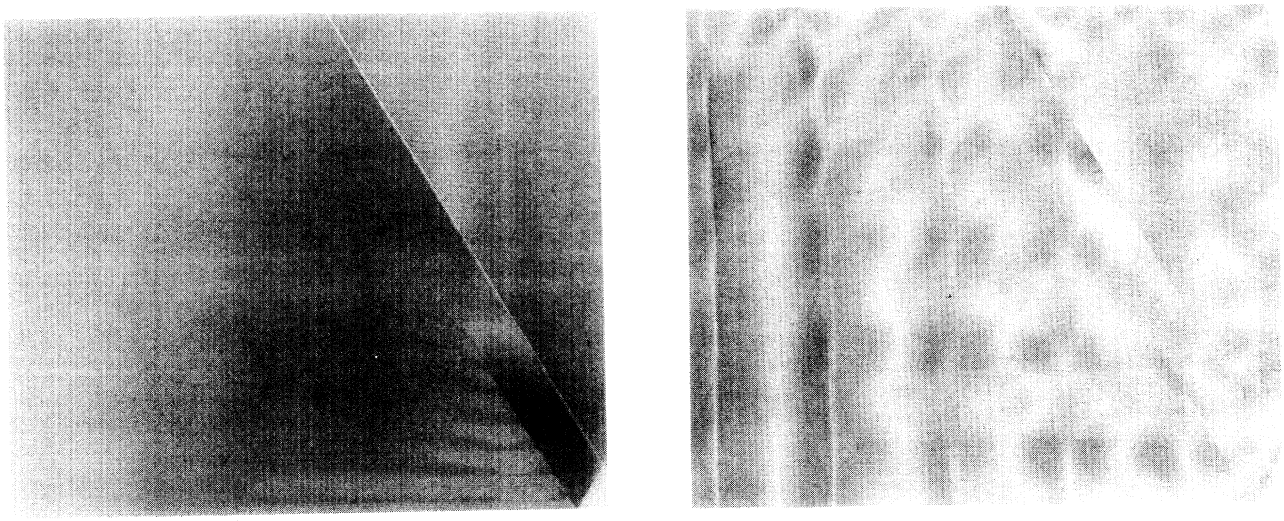

FIG. 8. The left picture shows the total displacement of the particles from their equilibrium positions 2.56 s after the start of the excitation. The right picture shows the velocity field for the system 2.56 s after the start of the excitation.

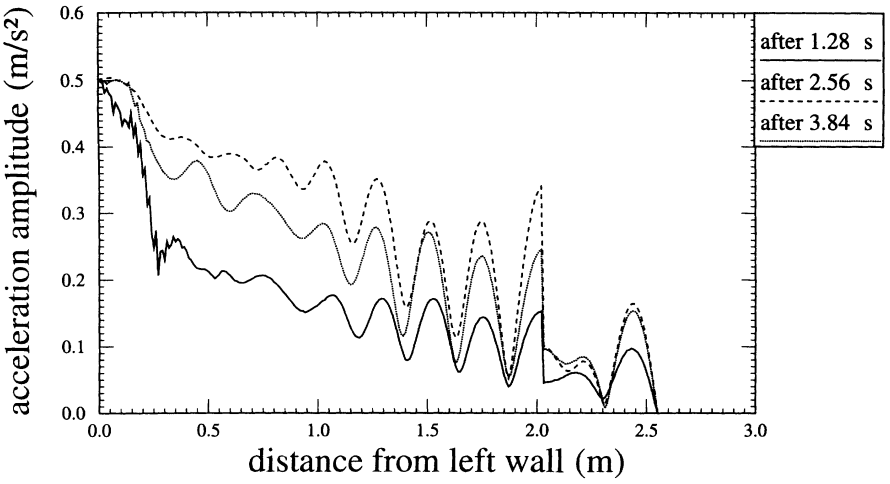

FIG. 9. The spatial distribution of the acceleration amplitudes in the 128th layer (counted from the surface). As one can see, there is a change in time. It looks as if there is a modulation only of the amplitudes, since the positions of the peaks do not change. This is currently under further investigation. Please note the sharp peak at a distance of approximately 2 m from the source; this is the position of the "fault line."

(even beyond the 3.8 s that I simulated in this case), just as has been observed by Liu and Nagel [1]. The existence of localized oscillations in a box full of grains has been postulated by recent numerical results for a very simplified model [2]; this is in agreement with the results shown here.

The effects of polydispersity can be seen in Figs. 10 and 11. Apart from being more irregular, the evolving patterns are very similar to the ones in the monodisperse case. In particular, figures depicting the phases of the vibrations in the x direction appear very similar; in both cases there is the same vertical structure. The fuzziness of the border of the areas of the same phase is due to the existence of the horizontal bonds from Fig. 1. These bonds form some finite chains along which the sound can travel faster than in other areas. This is also the reason for the absence of a well-defined wave front, as discussed in Sec. III for the polydisperse case. At the surface the effect of the horizontal bonds becomes even more pronounced for vibrations in the x direction. Small chains of particles which are connected by these bonds oscillate in a coherent fashion. A big difference, however, is that in the polydisperse case there are no apparent faults, because in this case the whole system expands. Just as in the monodisperse case, the velocity field is correlated to the phase field of the vibration in the x direction.

V. CONCLUSIONS AND COMPARISON OF THE RESULTS WITH REAL SAND

The results show that even for very simple cases the propagation of sound in granular assemblies under gravi-

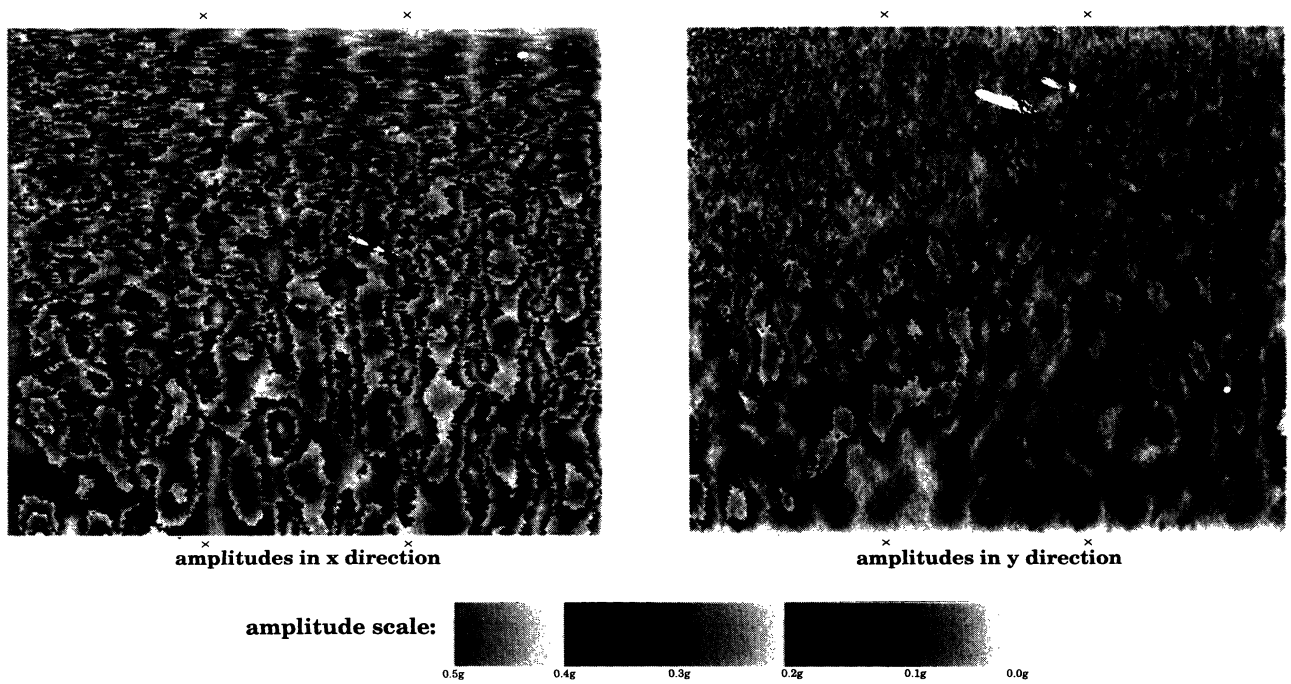

FIG. 10. The contour maps for the acceleration amplitudes for the polydisperse system 2.56 s after the start of the excitation. The left picture shows the acceleration amplitudes of the vibration in the x direction, the right the amplitudes in the y direction.

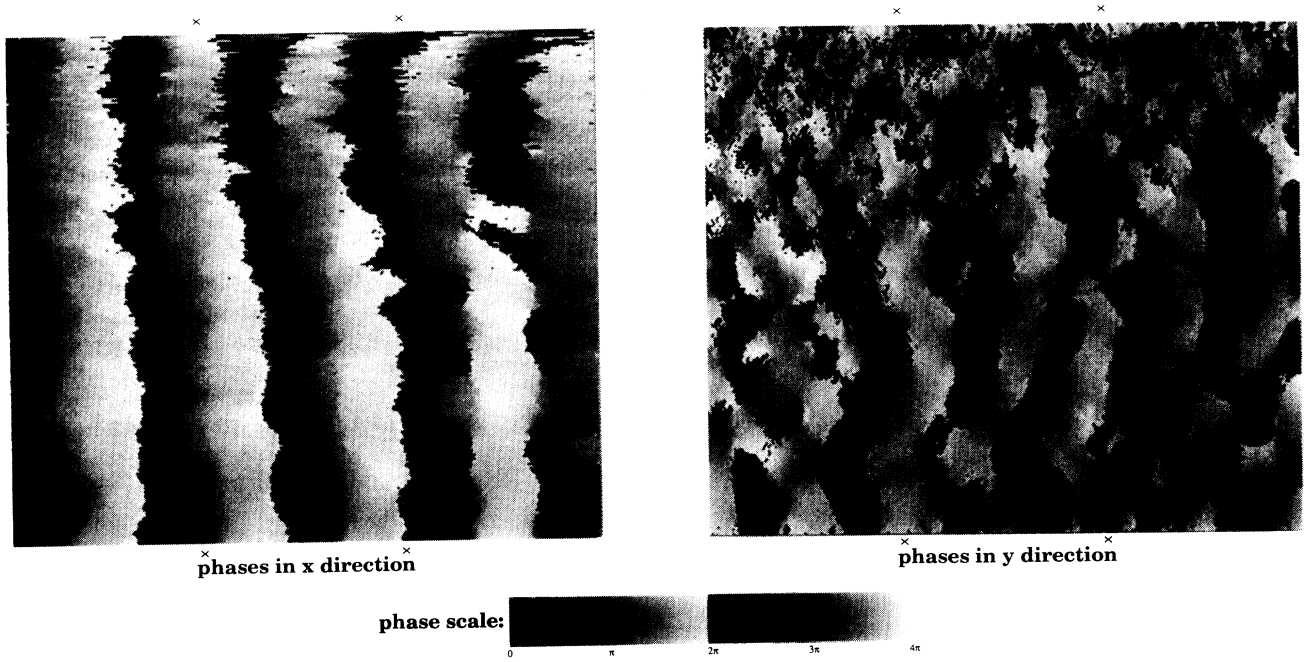

FIG. 11. The acceleration phases for the polydisperse system, 2.56 s after the start of the excitation. The left picture shows the phases of the vibration in the x direction, the right one shows the phases of the vibration in the y direction.

ty exhibit unexpected behavior.

The measured depth dependence of the wave propagation speed does not confirm the predicted power-law behavior, at least for the case of a regular packing of monodisperse spheres and for systems with slight polydispersity. Sound is propagated not only by the contact network which already exists in the equilibrated state, but also through a "contact network" which appears only when the system is distributed (i.e., an external vibration is given on the system). The shape and influence of this contact network on the sound propagation depends very much on the amplitude of the wave, thus making the wave propagation speed also dependent upon the amplitude.

For continuous excitation the spatial distribution of the acceleration amplitudes shows a very complicated behavior. The peaks of the amplitude are very localized even in the monodisperse case, showing that even the anisotropy introduced by gravitation is already enough to generate such complicated patterns.

When applying these numerical results to real granular assemblies, one has to consider that real sand has a rough surface and is not spherical. The effect on the horizontal stress distribution will not be much different from the effect of polydispersity, which can be seen in the right part of Fig. 1. The horizontal stress distribution for the polydisperse case is not depth dependent; if it were so, then the shape of the wave front for the polydisperse case would have been different from the one for the monodisperse case (see Fig. 2). However, the wave front travels a little bit faster for the polydisperse case, since some of the horizontal contacts are already closed. In this respect a system consisting of slightly nonspherical particles will behave very much like a system consisting of slightly polydisperse particles. For the case of rough surfaces or static friction, this effect will play a role when packing is very loose, in contrast to the dense packing used here. In this case a small excitation will be enough to rearrange the whole system permanently, i.e., it jumps from one stable state to another one. For very small excitations and an arrangement which is very near (or rather at) the stable state with the minimum energy, static fraction will not play a significant role. Such systems have been studied in this paper.

What remains to be shown is that it is possible to apply results obtained here to more general assemblies of granular materials.[12]

ACKNOWLEDGMENTS

I would like to thank Hans J. Herrmann, for many enlightening discussions, and also Gregory A. Kohring, Michael Leibig, Wolfgang Form, Peter Ossadnik, Gerald Ristow, Hans-Jürgen Tillemans, and the GMD (Gesellschaft für Mathematik und Datenverarbeitung) in St. Augustin for a grant of computer time on their CM2 computer.

[1] C. Liu and S. R. Nagel, Phys. Rev. Lett. **68**, 2301 (1992).
[2] M. Leibig, Phys. Rev. E **49**, 1647 (1994).
[3] J. D. Goddard, Proc. R. Soc. London, Ser. A **430**, 105 (1990).
[4] H. M. Jaeger and S. R. Nagel, Science **255**, 1523 (1992).
[5] L. Landau and E. Lifschitz, *Theoretische Physik, Band VII, Elastizitätstheorie* (Akademie Verlag, Berlin, 1965) pp. 33–39.

[6] J. A. C. Gallas, H. J. Herrmann, and S. Sokolowski, Phys. Rev. Lett. **69**, 1371 (1992).
[7] M. P. Allen and D. J. Tildesley, *Computer Simulation of Liquids* (Oxford University Press, Oxford, 1987).
[8] G. S. Grest, B. Dünweg, and K. Kremer, Comput. Phys. Commun. **55**, 269 (1989).
[9] D. C. Rapaport, Comput. Phys. Rep. **9**, 1 (1988).
[10] M. Schoen, Comput. Phys. Commun. **52**, 175 (1989).
[11] C. Liu and S. R. Nagel (unpublished).
[12] C. Liu and S. R. Nagel (unpublished).

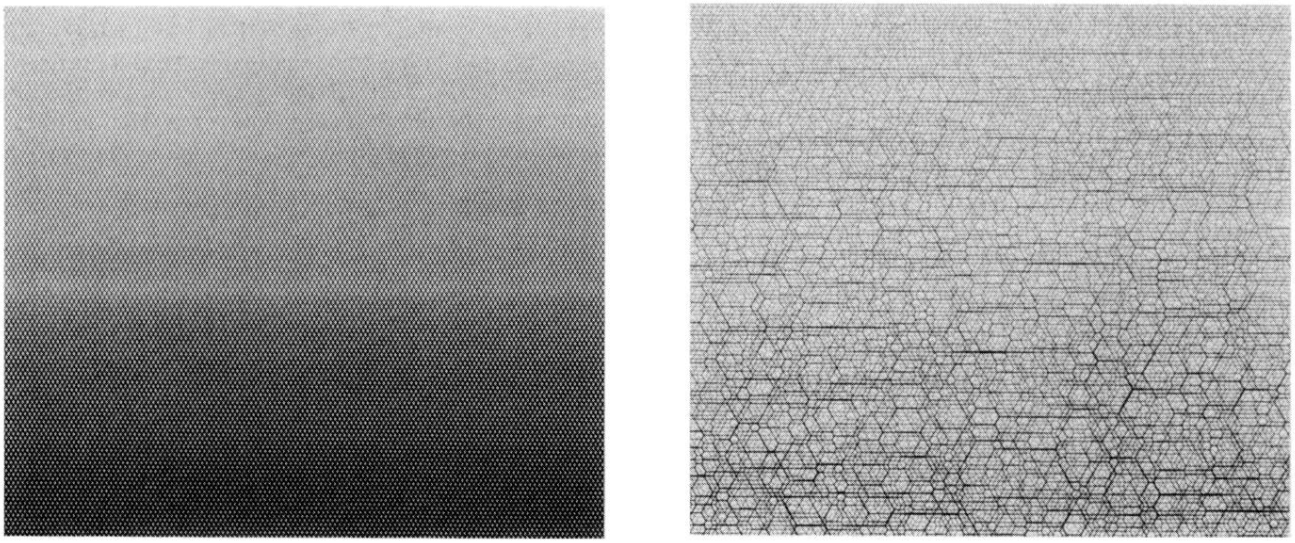

monodisperse

polydisperse

FIG. 1. These are excerpts from the contact network for an equilibrated 256×256 packing of spheres; the thickness codes the strength of the bonds. For the monodisperse case one can see that there are no horizontal bonds. Although the particles touch each other, there are no elastic forces between them. For the polydisperse case it is completely different; there are horizontal bonds.

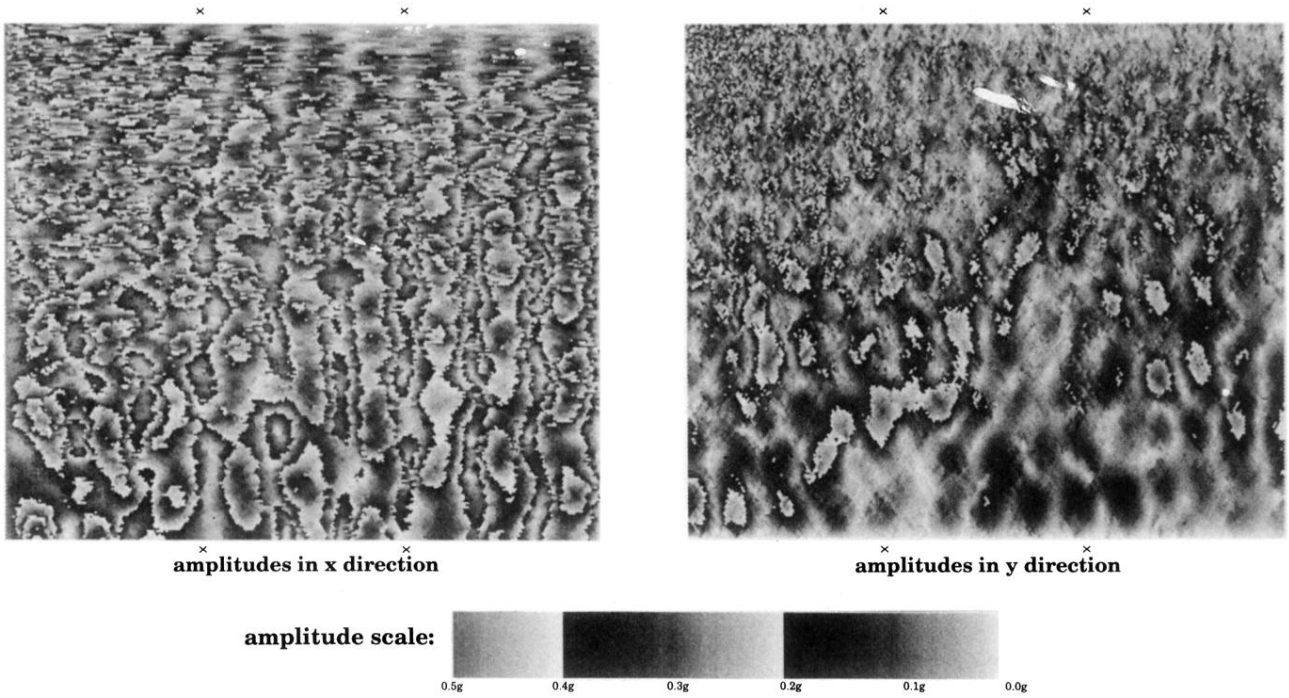

FIG. 10. The contour maps for the acceleration amplitudes for the polydisperse system 2.56 s after the start of the excitation. The left picture shows the acceleration amplitudes of the vibration in the x direction, the right the amplitudes in the y direction.

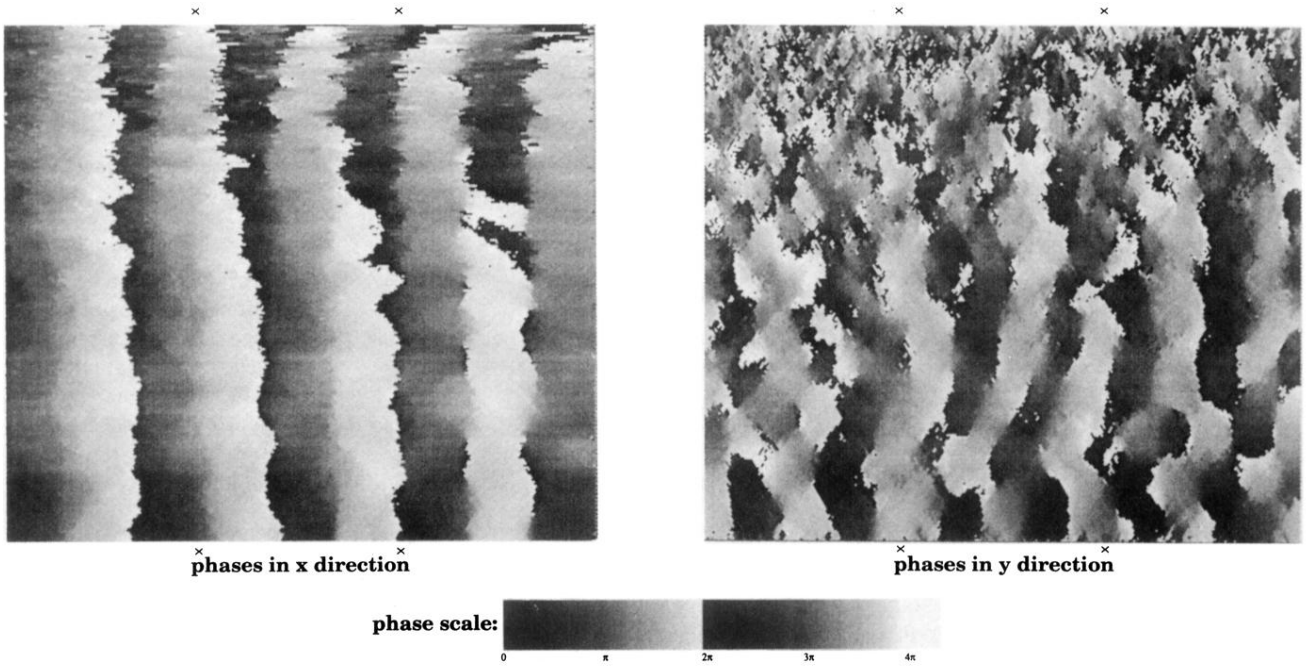

FIG. 11. The acceleration phases for the polydisperse system, 2.56 s after the start of the excitation. The left picture shows the phases of the vibration in the x direction, the right one shows the phases of the vibration in the y direction.

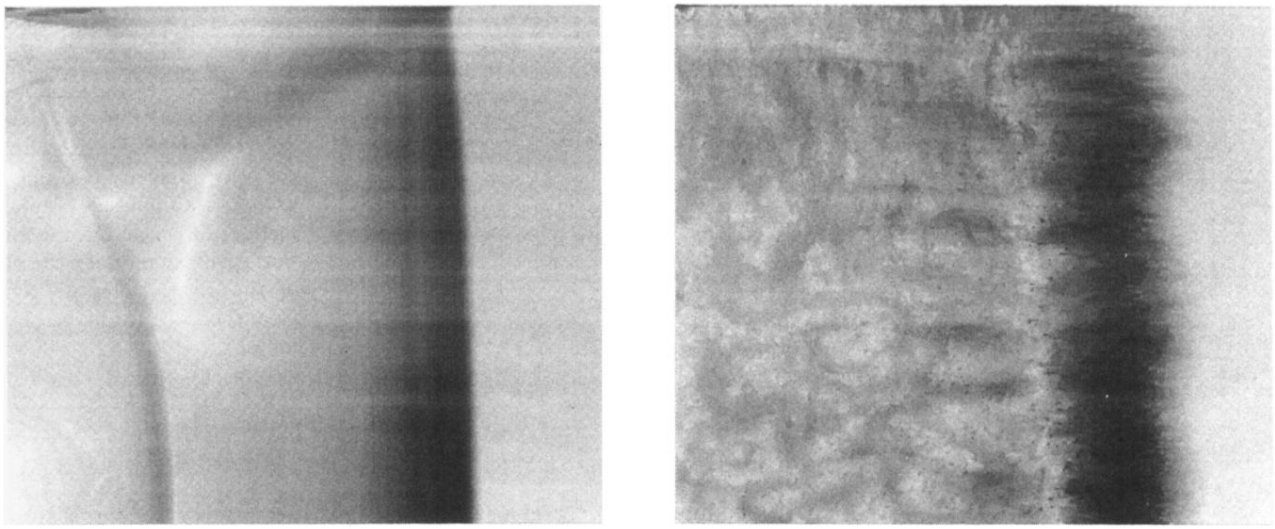

monodisperse polydisperse

FIG. 2. Here one can see the position of the wave front shortly before the wave hits the opposite wall in the system. The gray scales code the kinetic energy of the particles (dark means high kinetic energy). The amplitude is $0.01D$. The left figure shows the monodisperse case, and the right figure shows the polydisperse case. The main qualitative difference between these two figures is that in the polydisperse case the front is not smooth as in the monodisperse case. The structures behind the wave front are due to internal reflection of the wave. The secondary wave front in the monodisperse case is created at the beginning of the simulation and travels (due to its lower amplitude) much more slowly than the primary wave front.

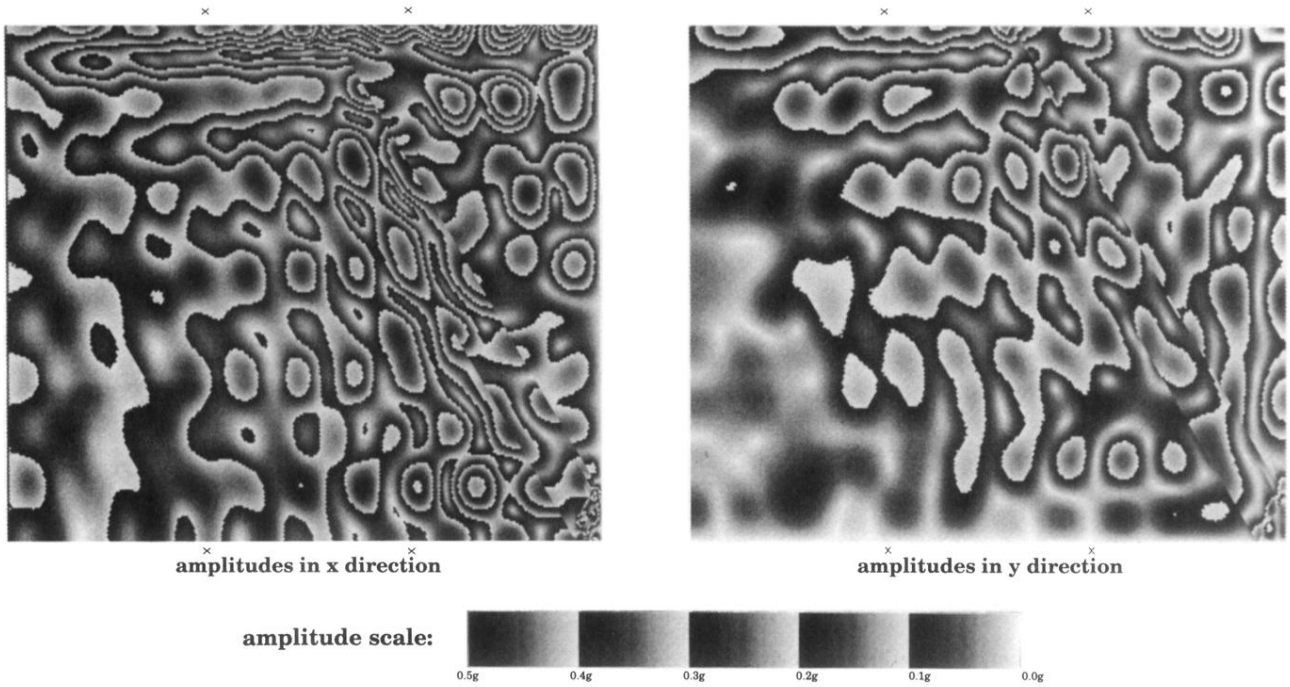

FIG. 6. The contour maps for the acceleration amplitudes of the monodisperse system 2.56 s after the start of the excitation. The left picture shows the acceleration amplitudes of the vibration in the x direction, and the right the amplitudes in the y direction.

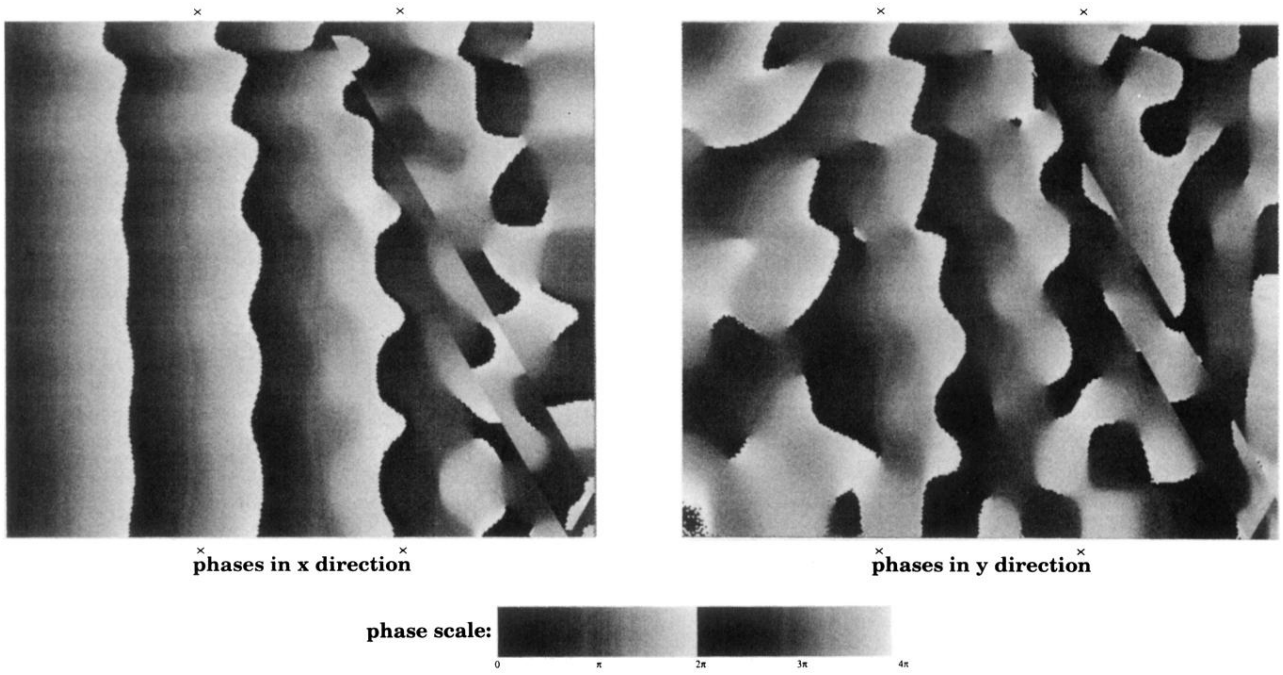

FIG. 7. The acceleration phases for the monodisperse system 2.56 s after the start of the excitation. The left picture shows the phases of the vibration in the x direction, the right one shows the phases of the vibration in y direction.

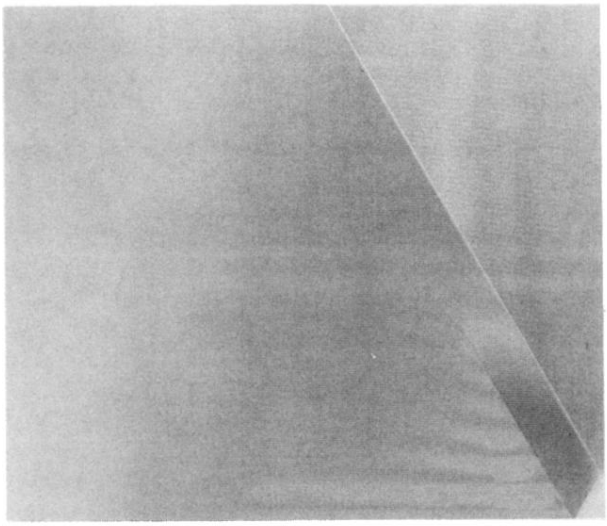

total displacement from the equilibrium position

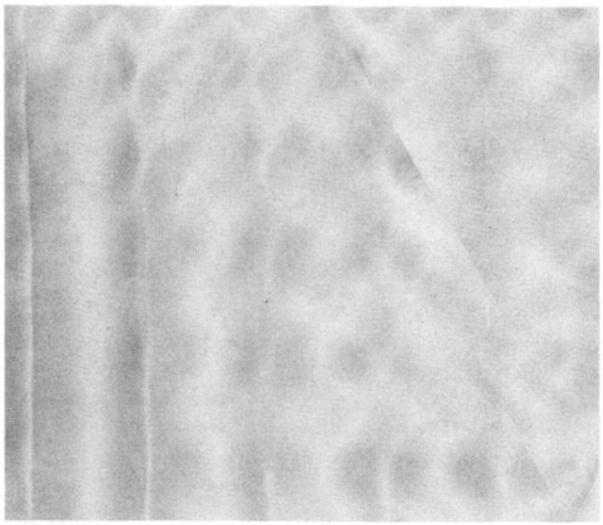

velocity field

FIG. 8. The left picture shows the total displacement of the particles from their equilibrium positions 2.56 s after the start of the excitation. The right picture shows the velocity field for the system 2.56 s after the start of the excitation.